Author's Accepted Manuscript

www.elsevier.com/locate/talanta

Paper surface modification strategies employing N-SBA-15/polymer composites in bioanalytical sensor design

Cristian M. Moreira, Maria L. Scala-Benuzzi, Eduardo A. Takara, Sirley V. Pereira, Matías Regiart, Galo J.A.A. Soler-Illia, Julio Raba, Germán A. Messina

PII: S0039-9140(19)30308-X
DOI: https://doi.org/10.1016/j.talanta.2019.03.051
Reference: TAL19729

To appear in: *Talanta*

Received date: 19 December 2018
Revised date: 12 March 2019
Accepted date: 13 March 2019

Cite this article as: Cristian M. Moreira, Maria L. Scala-Benuzzi, Eduardo A. Takara, Sirley V. Pereira, Matías Regiart, Galo J.A.A. Soler-Illia, Julio Raba and Germán A. Messina, Paper surface modification strategies employing N-SBA-15/polymer composites in bioanalytical sensor design, *Talanta,* https://doi.org/10.1016/j.talanta.2019.03.051

Paper surface modification strategies employing N-SBA-15/polymer composites in bioanalytical sensor design

Cristian M. Moreira[a], Maria L. Scala-Benuzzi[a], Eduardo A. Takara[a], Sirley V. Pereira[a], Matías Regiart[a], Galo J.A.A. Soler-Illia[b], Julio Raba[a], Germán A. Messina[a*]

[a]*INQUISAL. Departamento de Química, Universidad Nacional de San Luis. CONICET. Chacabuco 917. D5700BWS. San Luis, Argentina.*

[b]*Instituto de Nanosistemas, Universidad Nacional de San Martín, Av. 25 de Mayo 1021, San Martín, Buenos Aires, Argentina.*

[*]Corresponding author. German A. Messina INQUISAL. Departamento de Química, Universidad Nacional de San Luis. CONICET. Chacabuco 917. D5700BWS. San Luis, Argentina. (Tel.): +54 266 442 5385; (fax): +54 266 443 0224. messina@unsl.edu.ar

ABSTRACT

In this work, different paper surface modification strategies were compared to obtain an amine functionalized SBA-15 (N-SBA-15) composite for paper-based device development. The synthesized N-SBA-15 was characterized by N_2 adsorption-desorption isotherm, and infrared spectroscopy (FTIR), and it was incorporated to different polymer matrices (κ-carrageenan (CA), polyvinyl alcohol (PVA) and polyethylenimine (PEI)) for the development of the composite modified paper-based device. The retention, interactions, and morphology of the obtained composites were investigated by absorbance measurement,

FTIR and scanning electron microscopy (SEM), respectively. To demonstrate the applicability of the modified paper-based device, ascorbic acid (AA) quantification was carried out. Horseradish peroxidase (HRP) was immobilized onto the modified paper surface. HRP in the presence of H_2O_2 catalyzes the oxidation of 10-acetyl-3,7-dyhidroxyphenoxazine (ADHP) to highly fluorescent resorufin, which was measured by LIF detector. Thus, when AA was added to the solution, it decreases the relative fluorescence signal proportionally to the AA concentration. The linear range from 50 nmol L^{-1} to 1500 nmol L^{-1} and a detection limit of 15 nmol L^{-1} were obtained for AA quantitation. The obtained results allowed us to conclude that N-SBA-15/PEI composite could be considered an excellent choice for the paper-based device modification procedure due to its inherent simplicity, low cost, and sensitivity.

Keywords: Paper-based device; Fluorescence; Ascorbic Acid, N-SBA-15; Polyethylenimine.

1. Introduction

During the last years, the need for fast, sensitive, specific, automated and in situ detection methodologies has generated the development of easy-to-use and economical devices. Paper has drawn much interest as a potential support material for sensors in analytical and clinical chemistry because of its versatility, abundance, and low cost. Its fibrous and porous structure generates a high surface to volume ratio, increasing the immobilization surface compared to the traditional materials for device fabrication. Furthermore, the paper has other advantages such us its high biocompatibility, biodegradability and it is disposable material [1]. Besides, cellulose fibers can be readily

functionalized, thus changing properties such as hydrophilicity, permeability, and reactivity [2,3]. Taking into account these advantages, the development of paper-based analytical devices (PADs) has had significant growth. The most common detection methods coupled to for PADs are colorimetric [4] and electrochemical [5], although chemiluminescent and electrochemiluminescent [6] detections have been reported. Fluorescence detection represents an alternative option due to its high sensitivity and fast response time. Among the light sources, the light emitting diode (LED) induced fluorescence has recently called the interest because LEDs combine high stability, small size, low cost, broad spectra, long lifetime and low energy consumption [7–9].

In recent years, different materials have been incorporated into analytical biosensors as immobilization platform of specific reagents. Porous silica materials are commonly used as solid supports [10]. Among them, SBA-15 represents an attractive option for the paper surface coating. The use of this material has many benefits such as the increase of the surface to volume ratio which improves interactions between the biological and chemical reagents, decreasing the detection limits [11,12]. Moreover, SBA-15 can be functionalized with amino groups (N-SBA-15) for biomolecules immobilization. Compared with the commercial 3-aminopropyl modified controlled pore glass generally used as immobilization support, this mesoporous material presents an increased surface with uniform porous [13,14].

With the advent of PADs, polymers have been considered as a material with unique properties for paper surface treatment [15]. Among them, κ-carrageenan (CA), polyvinyl alcohol (PVA) and polyethylenimine (PEI) are interesting for the paper surface coating due to its polymer structure which allows improving the retention of different materials such as the N-SBA-15. In the first place, CA is a highly sulfated polysaccharide extracted from red

algae. The CA properties are influenced by the number and position of the ester sulfate groups and its content of 3,6-anhydrogalactose. These functional groups give the polymer anionic character to form ionic complexes with N-SBA-15 [16]. Second, PVA is a polymer with interesting properties, including adhesiveness, biocompatibility and lack of toxicity, which make it attractive for its use in surface modification [17]. PVA has a polymeric structure with the presence of hydroxyl functional group (-OH) which can form hydrogen bonds with N-SBA-15. Finally, PEI is a cationic branched polymer containing a high density of primary, secondary and tertiary amino groups, which can easily interact with functional groups of other molecules [18].

The objective of this work was to compare several modifications using N-SBA-15 composite and different polymer matrices for the construction of a novel paper-based device. To study the applicability of the obtained composites, they were functionalized with HRP to select the most suitable to be applied for AA quantitative determination in pharmaceutical formulations. The fluorescent product of the enzyme reaction in the H_2O_2 presence was detected by LIF, using excitation lambda at 535 nm and emission at 585 nm. Therefore, when AA is added to the solution, the relative fluorescence signal decreases proportionally to the increase of AA concentration. This process is due to AA is an electron donor and interferes with the HRP-catalyzed reaction [19]. The developed composite modified paper-based device shows to be an easy to use, disposable and inexpensive system that represents a promising tool for analytes detection.

2. Experimental

2.1. Materials and reagents

All the reagents were of analytical grade. Ascorbic acid, 10-Acetyl-3,7-dihydroxyphenoxazine (ADHP), enzyme horseradish peroxidase [EC 1.11.1.7] grade II, HCl (37 % w/w), pluronic P123 triblock copolymer (EO20-PO70-EO20), κ-carrageenan, polyvinyl alcohol, and polyethylenimine were purchased from Sigma-Aldrich (St. Louis, MO, USA). Glutaraldehyde (GLA) (25 % aqueous solution), hydrogen peroxide, ethanol, toluene, tetraethyl orthosilicate (TEOS 98 %), and 3-aminopropyl triethoxysilane (3-APTES) were purchased from Merck (Darmstadt, Germany). Paper-based devices were made with Whatman # 1 chromatographic paper. The aqueous solutions were prepared using purified water from a Milli-Q system. The pharmaceutical formulation samples were (1) Redoxon 1 g effervescent tablets (BAYER), (2) Redoxon 200 mg oral drops (BAYER), (3) Vitamin C injectable (DAWER), (4) 1 g vitamin C powder (ISA), (5) 500 mg vitamin C tablets (LAFARMEN).

2.2. Instruments

Fluorescent measurements were performed using a synchronized video microscope SVM340TM (LabSmith, Livermore, California, USA). All pH measurements were made with an Orion Research Inc. (Orion Research Inc., Cambridge, MA, USA) Model EA 940 equipped with a glass combination electrode (Orion Research Inc.). The paper device was printed by a Xerox Phaser printer from XEROX (ARG). PDC-32G device (Micro Technology Co. Ltd., USA) was used for the oxygen plasma treatment. Scanning electron microscope (SEM) images were taken on a Carl Zeiss NTS SUPRA 40; The TEM micrographs were taken on a Zeiss EM109T. Infrared (FTIR) spectroscopic measurements were obtained in a Spectrum 65 FTIR spectrometer Perkin Elmer, in a region from 4000 to 800 cm^{-1}. Textural characterization was carried out by N_2 adsorption-desorption isotherms

at 77 K using a manometric adsorption equipment (ASAP 2000, Micromeritics), where the samples were previously degassed at 250 °C for 12 h, up to a residual pressure smaller than 3 Pa.

2.3. Paper surface modification with N-SBA-15

A reaction microzone was made in the paper to generate a hydrophobic barrier. A 6 mm-diameter circular pattern was designed using the graphic software Corel Draw 9 and printed with wax on a Whatman # 1 filter paper by the Xerox ColorQube 8870 wax printer. Later, the papers were exposed to 90 °C for 5 min to create a hydrophobic barrier.

The SBA-15 was synthesized and, subsequently, functionalized with amino groups following previous works [20,21] (these methods are described in the supplementary material, SM1). Besides, SBA-15 and N-SBA-15 were characterized by N_2 adsorption-desorption isotherm at 77 K (see supplementary material SM3).

The retention of N-SBA-15 on the paper microzone surface, four different methodologies were studied:

A) The paper surface was oxidized by oxygen plasma treatment [22] to generate aldehyde groups in the cellulose. Then, 20 µL of N-SBA-15 was added to the modified paper and left to react for 30 min in a humid chamber and later, it was dried by an N_2 flow.

B) 20 µL of 0.05 % CA solution were added to the unmodified paper microzone and exposed to a N_2 flow for 30 s. Then, 20 µL of N-SBA-15 suspension was incorporated and dried under N_2 flow. The N-SBA-15 retention was achieved by the interaction between the polyanion and the amino groups of N-SBA-15. For this purpose, the pKa of both species was evaluated, selecting an optimal pH value of 6.00 [21, 22].

C) A microzone was modified without plasma treatment by adding 20 µL of 0.05 % PEI solution and then exposed to a N_2 flow for 30 s. The incorporation of PEI generated a higher number of amino groups on the paper surface, allowing for greater interaction between PEI and N-SBA-15.

D) 20 µL of 0.05 % PVA solution was added to the unmodified paper microzone, and dried under N_2 flow for 30 s. After that, 20 µL of N-SBA-15 suspension was incorporated and exposed to a N_2 flow until dry. The paper modification was performed by the addition of PVA to generate interactions between the hydroxyl groups present in the polymer and the N-SBA-15 amino groups.

For all the modifications the polymers (see supplementary material SM2) and N-SBA-15 concentrations, the N_2 flow and the drying times were normalized. The modified papers with N-SBA-15 were immersed in 1 mL of GLA 5 % w/w solution (acetone medium, pH 8.00, except PVA which was worked in acid medium) for 2 h at room temperature. After three washes with 0.01 mol L^{-1} sodium phosphate buffer (PBS) pH 7.00. The existing interactions generated in the N-SBA-15 retention for the different polymers were studied by FTIR.

2.4. Enzyme immobilization

HRP was immobilized on the modified paper surfaces (described in section 2.3). In brief, 5 µL of HRP (dilution 1:100 in 0.01 mol L^{-1} PBS pH 7.00) was incubated for 30 min at 37 °C on each modified paper surface. The immobilized enzyme preparation was finally washed three times with PBS 0.01 mol L^{-1} pH 7.00 and stored in the same buffer at 4 °C.

2.5. Enzymatic response study

The enzymatic response of the modified and functionalized with HRP paper microzones was studied by spectrophotometry. A chromophore solution, which was composed of 40 μg mL^{-1} o-phenylenediamine dihydrochloride (OPD) and 1 mmol L^{-1} H_2O_2 solution in citrate buffer pH 5.00, was added to each modified paper. After 3 min of incubation time, a 0.5 N H_2SO_4 solution was used as a stopper solution. Then, the absorbance was measured at 490 nm. The assay was carried out at a saturation concentration of the enzyme to compare the obtained signals.

The enzymatic response obtained by the different modification procedures tested revealed remarkably higher signals for N-SBA-15/PEI with immobilized HRP when compared with that obtained by the other tested modification procedures. Accordingly, this modification procedure was selected as the best option for the paper surface modification.

2.6. Ascorbic acid quantification in pharmaceutical samples

The developed paper-based devices were applied to the AA determination in pharmaceutical formulations. For tablets presentations, ten tablets were powdered, and the weight equivalent to one tablet was transferred to a 100 mL flask. In injectable, powder and the oral-drop preparations, all the content was placed inside a 100 mL flask. The flasks were sonicated and, finally, the volume was completed with phosphate-citrate buffer (0.1 M, pH 5.00) to adjust the samples at the optimum pH measurement.

AA determination was carried out by LIF detection. The procedure involves the following steps. Firstly, 5 μL of a mixture solution containing AA sample or standard, 1 mmol L^{-1} H_2O_2, and 0.75 μmol L^{-1} ADHP (in 0.1 mol L^{-1} phosphate-citrate buffer pH 5.00) was added to the modified paper device. HRP, in the presence of H_2O_2 catalyzes the

oxidation of ADHP to highly fluorescent resorufin, which was measured by LIF detection (excitation lambda at 535 nm and emission at 585 nm). When AA was added, it reduced the H_2O_2 to H_2O, decreasing the relative fluorescence signal of resorufin, proportionally to the increase of AA concentration.

3. Results and discussion

3.1 Characterization of SBA-15 and N-SBA-15

SBA-15 and N-SBA-15 were characterized by FTIR and N_2 adsorption-desorption. Figure 1 shows the FTIR measurements of SBA-15 and N-SBA-15. Both materials present the characteristic bands of the inorganic framework: Si-O-H (960 cm^{-1}), Si-CH_2-R (1220 cm^{-1}) and Si-O-Si (800 cm^{-1}) [23]. The Si-O-H band in N-SAB-15 turns into a shoulder, which indicates the presence of aminosilane groups. The most significant signal is the band corresponding to the asymmetric flexion of $N\text{-}H^+$ at 1560 cm^{-1} for the N-SBA-15. Moreover, the signals in the 2800-3000 cm^{-1} and 3000-3500 cm^{-1} zones show an increase in the bands attributed to the vibrations -C-H and the stretch N-H superimposed on the water bands, respectively, which confirms the presence of organic groups in SBA-15 [24]. The nitrogen adsorption-desorption isotherm at 77 K for SBA-15 and N-SBA-15 are shown in the supplementary material. The specific surface areas were calculated by the Brunauer, Emmet, and Teller (BET) method, obtaining a value of 474.2 $m^2\ g^{-1}$ for SBA-15 and 221.5 $m^2\ g^{-1}$ for N-SBA-15. The pore diameter distributions were estimated by the BJH method using desorption branch data, and the obtained average pore sizes were 5.4 nm for SBA-15 and 4.6 nm for N-SBA-15.

3.2. Study of paper surfaces modified with N-SBA-15 composites

The N-SBA-15 was incorporated to paper microzones to increase the immobilization surface. Figure 2 shows the SEM micrographs of modified paper with N-SBA-15/CA (a), N-SBA-15/PVA (b) and N-SBA-15/PEI (c). The analysis of the SEM micrographs did not register significant differences for the proposed methodologies. Excellent dispersion of the mesoporous material in PEI and PVA polymeric matrices were observed, while N-SBA-15/CA presented a lesser dispersion. Figure 3 a and b show a paper modified with N-SBA-15/PEI. Particles of 500 nm, approximately, can be observed in the paper surface. These images prove that the modification with N-SBA-15 was performed. Also, the typical channel-like structure was confirmed by TEM (Fig. 3c).

The infrared spectra were obtained for the modified papers to study the interactions between polymers and N-SBA-15. In Figure 4, the FTIR obtained spectra are shown. The CA spectrum (Fig. 3a) shows the characteristic bands of the polymer [25] while N-SBA-15/CA spectrum shows an increase of the band at 3300 cm^{-1} indicating the presence of -NH_2. Besides, a shift from 1560 to 1530 cm^{-1} of the primary amines band of the N-SBA-15 is observed, and a decrease in the band intensity at 1250 cm^{-1} which is attributed to the presence of sulfate ester groups. These changes confirm the generation of the ionic complex between the amino groups of SBA-15 and the sulfate groups of CA [26]. Nevertheless, the signal at 1745 cm^{-1} belonging to the aldehyde groups is overlapped with the band from 1760 to 1570 cm^{-1}, indicating a low proportion of free aldehydes. This could be attributed to the pH of the reaction medium.

Figure 4b shows the spectrum of PVA [27] and N-SBA-15/PVA composite. A widening and shifting of the signal in the region from 3000 to 3700 cm^{-1} is observed in the composite, attributed to the decrease of -OH groups (reaction with GLA) and the H-bridge interactions present in the matrix, respectively. In addition, a strong increase in the

absorption in the range of 1750 to 1500 cm^{-1} is observed corresponding to an overlap of the C=O groups, primary and secondary amines signals. The observed interactions revealed covalent bindings (PVA-GLA-PVA, PVA-GLA-N-SBA-15) and the presence of residual aldehyde groups GLA.

Finally, the spectra obtained for PEI and N-SBA-15/PEI (Fig. 4c) are shown. The characteristic bands of PEI were observed in both spectra [28,29]. The crosslinking of PEI and the bond of N-SBA-15 with GLA produce increases in the absorption at 3500 cm^{-1} and 1655 cm^{-1} due to the amine (NH_2) and imine (N=C) bonds, respectively [30]. Also, a peak at 1720 cm^{-1} is observed, attributed to free aldehyde bonds. These changes in the spectrum indicate that the crosslinking with GLA generated the covalent binding between N-SBA-15 and PEI, providing reactive aldehyde groups on the surface.

3.3. Enzymatic response

In order to improve the performance of the developed paper-based devices, the enzymatic responses for each composite were compared. Figure 5a shows the obtained signals expressed as a percentage related to the signal obtained by the plasma treated paper (P-P). The N-SBA-15/PEI composite showed the highest response due to that HRP is covalently immobilized both onto the N-SBA-15 and PEI through GLA. In the case of N-SBA-15/CA composite, the low response is attributed to the deprotonation of the N-SBA-15 amino groups during the immobilization reaction of the HPR. This affects the formation of the ionic complex and the free aldehyde proportion. The N-SBA-15/PVA composite presented a low response, which could be attributed to the strong H-bonds interaction between the -OH of PVA and -NH_2 groups of N-SBA-15, decreasing the active sites available for the immobilization of HRP.

Considering the features previously described for each modification procedure and the intensity of the displayed signals, N-SBA-15/PEI composite represents an excellent strategy for the design and construction of the composite modified paper device. Regarding the signal intensity, this device generates a large increase in the signal of 8 times compared to the P-P.

Finally, the optimum N-SBA-15 concentration was studied modifying paper microzones with 0.05 % PEI and various concentrations (0.3 to 0.7 %) of the mesoporous material. Then, a saturation concentration of HRP was immobilized and the absorbance method was carried out. Figure 5b shows the enzymatic response indicating a maximum ratio for a concentration of 0.5 %. For these reasons, a paper-based device modified with 0.5 % N-SBA-15, and 0.05 % PEI was developed for the ascorbic acid determination.

3.4. Analytical performance for AA quantification using N-SBA-15/PEI modified paper device

The N-SBA-15/PEI modified paper device was tested for AA determination as shown in the schematic representation in Fig. 6. For this purpose, the experimental variables that affect the paper-based device performance were optimized (see Figure S3, SM4). The working pH of 0.1 mol L^{-1} phosphate-citrate buffer in the pH range from 2.00 to 10.00 was evaluated. The optimal response was observed with a value of pH 5.00. The H_2O_2 concentration was tested between 0.1 to 1.5 mmol L^{-1}, and the optimal signal was found at a concentration of 1 mmol L^{-1} H_2O_2. Also, a concentration range from 0.1 to 1.25 µmol L^{-1} of ADHP was studied, exhibiting a maximum response value at 0.75 µmol L^{-1}. Another parameter analyzed was the enzyme concentration. This factor was evaluated using

250 µL HRP in 0.01 mol L^{-1} PBS pH 7.00 at 1:50, 1:100, 1:250, 1:500, and 1:1000; the optimal HRP dilution was 1:100.

The linearity and range for the quantification were studied under the optimized conditions. Standard solutions containing AA concentration in the range from 10 to 3000 nmol L^{-1} were used. A linear relation from 50 nmol L^{-1} to 1500 nmol L^{-1} was obtained for the method. The linear regression was described by the following equation: RFU = 3487.56–2.27 [AA] with a correlation coefficient r = 0.997. Furthermore, the limit of detection (LOD) was 15 nmol L^{-1}, according to IUPAC consideration. The precision was evaluated with the 400 nmol L^{-1} AA standard. To obtain the variation coefficients (VC), the method was carried out with the standards 5 times in a day, and they were repeated for 3 consecutive days. The paper-based device showed values of VC within-assay below 4.7 % and VC between-assay values below 5.3 %. Recovery studies were performed (SM5) and the obtained recovery values ranged from 98.8 % to 101.5 % and the accuracy for AA was 1.5 %. Therefore, the proposed method had good accuracy for AA quantification. Furthermore, the developed paper-based device was applied to five commercial preparations; the corresponding results are shown in Table 1.

The stability of our device was studied by performing repetitive calibration graphs in the above-mentioned concentrations range after storage of the paper-based device in PBS buffer, at 4 ºC. Figure 7 shows the mean value of the slopes of three successive calibration plots as the central value and the mean values of the slopes of the three-consecutive calibration. The upper and lower limits of control were set at ± 3 standard deviations of the central value. As can be appreciated, our method yielded mean slope values within the established limits for 30 days.

Moreover, the developed method was compared with other recently reported methods for the AA determination by fluorescence (Table 2). This analytical method has advantages over the previously reported. The detection limit achieved by our method is lower than the obtained by the reported ones. Furthermore, we present a device which has the advantages of using paper as supporting material. Besides, our system uses the amino-functionalized SBA-15 platform for immobilizing the HRP, which increased the specificity. Finally, our sensor has the potential to answer the growing needs for analytical tools that fulfill requirements such as low cost, sensitivity and short analysis time.

Conclusions

This article describes the comparison of several methodologies for paper surface modifications whit N-SBA-15 and different polymer matrices (CA, PVA, and PEI). Among the obtained composites, N-SBA-15/PEI displayed the higher signal response, providing an excellent platform for the disposable paper biosensors construction. N-SBA-15 nanoporous structure increased the biomolecules immobilization capacity of the sensing surface. PEI plays a fundamental role by establishing strong interactions with the mesoporous material and contributing with NH_2 groups for the recognition agent incorporation. The obtained composite paper platform was covalently functionalized with HRP. To demonstrate the applicability of N-SBA-15/PEI modified paper-based device, AA was quantified in pharmaceutical formulations. The proposed device exhibited a low detection limit (15 nmol L^{-1}), stability and inexpensive fabrication. To conclude, our method represents a promising tool whose usefulness could easily be extended to the detection of different relevant biomolecules.

Acknowledgements

The authors wish to thank the financial support from the Universidad Nacional de San Luis (PROICO-1512-22/Q232), the Agencia Nacional de Promocion Cientifica y Tecnológica and the Consejo Nacional de Investigaciones Cientificas y Tecnicas (CONICET) (PICT-2015-2246, PICT 2015-3526, PICT-2015-1575, PICT-2014-1184, PICT-2013-3092, PICT-2013-2407).

References

[1] T. Akyazi, L. Basabe-Desmonts, F. Benito-Lopez, Review on microfluidic paper-based analytical devices towards commercialisation, Anal. Chim. Acta. 1001 (2018) 1–17.

[2] Y. Xu, M. Liu, N. Kong, J. Liu, Lab-on-paper micro- and nano-analytical devices: Fabrication, modification, detection and emerging applications, Microchim. Acta. 183 (2016) 1521–1542.

[3] S. Ahmed, M.P.N. Bui, A. Abbas, Paper-based chemical and biological sensors: Engineering aspects, Biosens. Bioelectron. 77 (2016) 249–263.

[4] G.G. Morbioli, T. Mazzu-Nascimento, A.M. Stockton, E. Carrilho, Technical aspects and challenges of colorimetric detection with microfluidic paper-based analytical devices (μPADs) - A review, Anal. Chim. Acta. 970 (2017) 1–22.

[5] J. Adkins, K. Boehle, C. Henry, Electrochemical paper-based microfluidic devices, Electrophoresis. 36 (2015) 1811–1824.

[6] L. Ge, J. Yu, S. Ge, M. Yan, Lab-on-paper-based devices using chemiluminescence and electrogenerated chemiluminescence detection, Anal. Bioanal. Chem. 406 (2014) 5613–5630.

[7] H. Ji, Y. Wu, Z. Duan, F. Yang, H. Yuan, D. Xiao, Sensitive determination of sulfonamides in environmental water by capillary electrophoresis coupled with both silvering detection window and in-capillary optical fiber light-emitting diode-induced fluorescence detector, Electrophoresis. 38 (2017) 452–459.

[8] J. Mazina, A. Spiljova, M. Vaher, M. Kaljurand, M. Kulp, A rapid capillary electrophoresis method with LED-induced native fluorescence detection for the analysis of cannabinoids in oral fluid, Anal. Methods. 7 (2015) 7741–7747.

[9] W. Gu, W., Huang, J., & Tan, LED induced transmitted fluorescence detector integrated in microfluidic cell chip, Int. J. Nanotechnol. 22 (2015) 742–752.

[10] M. Moritz, M. Geszke-Moritz, Mesoporous materials as multifunctional tools in biosciences: principles and applications, Mater. Sci. Eng. C. Mater. Biol. Appl. 49 (2015) 114–151.

[11] P. Wang, M. Li, F. Pei, Y. Li, Q. Liu, Y. Dong, Q. Chu, H. Zhu, An ultrasensitive sandwich-type electrochemical immunosensor based on the signal amplification system of double-deck gold film and thionine unite with platinum nanowire inlaid globular SBA-15 microsphere, Biosens. Bioelectron. 91 (2017) 424–430.

[12] X. Li, Y. Li, R. Feng, D. Wu, Y. Zhang, H. Li, B. Du, Q. Wei, Ultrasensitive electrochemiluminescence immunosensor based on Ru(bpy)32+and Ag nanoparticles doped SBA-15 for detection of cancer antigen 15-3, Sensors Actuators, B Chem. 188 (2013) 462–468.

[13] M.A. Seia, S.V. Pereira, C.A. Fontan, I.E. De Vito, G.A. Messina, J. Raba, Laser-induced fluorescence integrated in a microfluidic immunosensor for quantification of human serum IgG antibodies to Helicobacter pylori, Sensors Actuators, B Chem. 168 (2012).

[14] S. V. Pereira, J. Raba, G.A. Messina, IgG anti-gliadin determination with an immunological microfluidic system applied to the automated diagnostic of the celiac disease, Anal. Bioanal. Chem. 396 (2010) 2921–2927.

[15] C.M. Wang, C.Y. Chen, W.S. Liao, Paper-polymer composite devices with minimal fluorescence background, Anal. Chim. Acta. 963 (2017) 93–98.

[16] S. Shankar, J.P. Reddy, J.W. Rhim, H.Y. Kim, Preparation, characterization, and antimicrobial activity of chitin nanofibrils reinforced carrageenan nanocomposite films, Carbohydr. Polym. (2015).

[17] F.M. Plieva, M. Karlsson, M.R. Aguilar, D. Gomez, S. Mikhalovsky, I.Y. Galaev, B. Mattiasson, Pore structure of macroporous monolithic cryogels prepared from poly(vinyl alcohol), J. Appl. Polym. Sci. 100 (2006) 1057–1066.

[18] W.-J. Son, J.-S. Choi, W.-S. Ahn, Adsorptive removal of carbon dioxide using polyethyleneimine-loaded mesoporous silica materials, Microporous Mesoporous Mater. 113 (2008) 31–40.

[19] G.A. Messina, A.A.J. Torriero, I.E.D. Vito, J. Raba, Continuous-flow/stopped-flow system for determination of ascorbic acid using an enzymatic rotating bioreactor, Talanta. 64 (2004) 1009–1017.

[20] T.P.B. Nguyen, J.W. Lee, W.G. Shim, H. Moon, Synthesis of functionalized SBA-15 with ordered large pore size and its adsorption properties of BSA, Microporous Mesoporous Mater. 110 (2008) 560–569.

[21] a S.M. Chong, X.S. Zhao, Functionalization of SBA-15 with APTES and characterization of functionalized materials, J. Phys. Chem. B. 107 (2003) 12650–12657.

[22] M. Zhao, H. Li, W. Liu, Y. Guo, W. Chu, Plasma treatment of paper for protein

immobilization on paper-based chemiluminescence immunodevice, Biosens. Bioelectron. 79 (2016) 581–588.

[23] P. Innocenzi, Infrared spectroscopy of sol – gel derived silica-based films : a spectra-microstructure overview, 316 (2003) 309–319.

[24] M.L. Scala-Benuzzi, E.A. Takara, M. Alderete, G.J.A.A. Soler-Illia, R.J. Schneider, J. Raba, G.A. Messina, Ethinylestradiol quantification in drinking water sources using a fluorescent paper based immunosensor, Microchem. J. 141 (2018) 287–293.

[25] V. Paşcalau, V. Popescu, G.L. Popescu, M.C. Dudescu, G. Borodi, A. Dinescu, I. Perhaița, M. Paul, The alginate/k-carrageenan ratio's influence on the properties of the cross-linked composite films, J. Alloys Compd. 536 (2012) 418–423.

[26] G.R. Mahdavinia, A. Mosallanezhad, M. Soleymani, M. Sabzi, Magnetic- and pH-responsive κ-carrageenan/chitosan complexes for controlled release of methotrexate anticancer drug, Int. J. Biol. Macromol. 97 (2017) 209–217.

[27] H.S. Mansur, C.M. Sadahira, A.N. Souza, A.A.P. Mansur, FTIR spectroscopy characterization of poly (vinyl alcohol) hydrogel with different hydrolysis degree and chemically crosslinked with glutaraldehyde, Mater. Sci. Eng. C. 28 (2008) 539–548.

[28] S. Inphonlek, N. Pimpha, P. Sunintaboon, Synthesis of poly(methyl methacrylate) core/chitosan-mixed-polyethyleneimine shell nanoparticles and their antibacterial property, Colloids Surfaces B Biointerfaces. 77 (2010) 219–226.

[29] P. Srinivasa Rao, B. Smitha, S. Sridhar, A. Krishnaiah, Preparation and performance of poly(vinyl alcohol)/polyethyleneimine blend membranes for the dehydration of 1,4-dioxane by pervaporation: Comparison with glutaraldehyde cross-linked membranes, Sep. Purif. Technol. 48 (2006) 244–254.

[30] M.M. Beppu, R.S. Vieira, C.G. Aimoli, C.C. Santana, Crosslinking of chitosan membranes using glutaraldehyde: Effect on ion permeability and water absorption, J. Memb. Sci. 301 (2007) 126–130.

[31] H. Liu, W. Na, Z. Liu, X. Chen, X. Su, A novel turn-on fluorescent strategy for sensing ascorbic acid using graphene quantum dots as fluorescent probe, Biosens. Bioelectron. 92 (2017) 229–233.

[32] Y. Hu, L. Zhang, X. Geng, J. Ge, H. Liu, Z. Li, A rapid and sensitive turn-on fluorescent probe for ascorbic acid detection based on carbon dots–MnO_2 nanocomposites, Anal. Methods. 9 (2017) 5653–5658.

[33] W. Na, Z. Qu, X. Chen, X. Su, A turn-on fluorescent probe for sensitive detection of sulfide anions and ascorbic acid by using sulfanilic acid and glutathione functionalized graphene quantum dots, Sensors Actuators, B Chem. 256 (2018) 48–54.

[34] X. Gong, Y. Liu, Z. Yang, S. Shuang, Z. Zhang, C. Dong, An “on-off-on” fluorescent nanoprobe for recognition of chromium(VI) and ascorbic acid based on phosphorus/nitrogen dual-doped carbon quantum dot, Anal. Chim. Acta. 968 (2017) 85–96.

[35] H. Rao, Y. Gao, H. Ge, Z. Zhang, X. Liu, Y. Yang, Y. Liu, W. Liu, P. Zou, Y. Wang, X. Wang, H. He, X. Zeng, An “on-off-on” fluorescent probe for ascorbic acid based on Cu-ZnCdS quantum dots and α-MnO2 nanorods, Anal. Bioanal. Chem. 409 (2017) 4517–4528.

Fig. 1 FTIR measurements of SBA-15 and N-SBA-15.

Fig. 2 SEM micrograph of paper microzone modified with (a) N-SBA-15/CA, (b) N-SBA-15/PVA and (c) N-SBA-15/PEI.

Fig. 3 SEM (a, b) and TEM (c) of the paper modified with N-SBA-15/PEI.

Fig. 4 FTIR spectrum of (a) N-SBA-15/CA and CA, (b) N-SBA-15/PVA and PVA, and (c) N-SBA-15/PEI and PEI.

Fig. 5 Enzymatic response for (a) different composites with and without N-SBA-15, (b) different concentration of N-SBA-15 whit 0.05 % of PEI.

Fig. 6 Analytical procedure for AA determination in pharmaceutical formulation samples.

Fig. 7 Control chart constructed for our device in PBS buffer, at 4 ºC. Data shown correspond to the mean values of the slopes of three consecutive calibration plots.

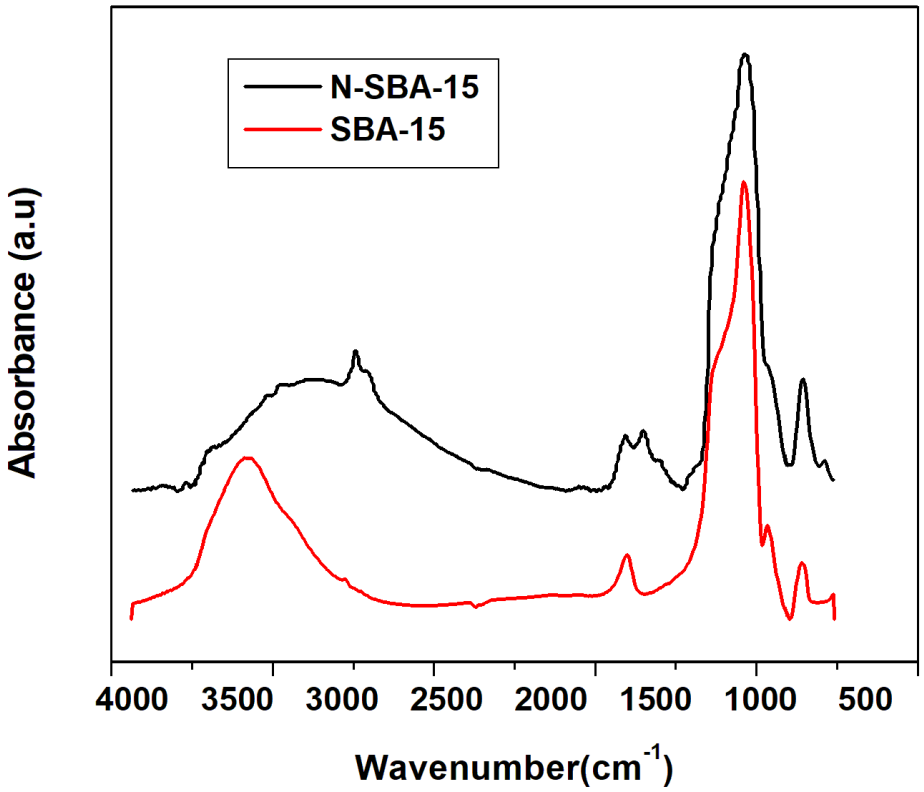

Fig. 1

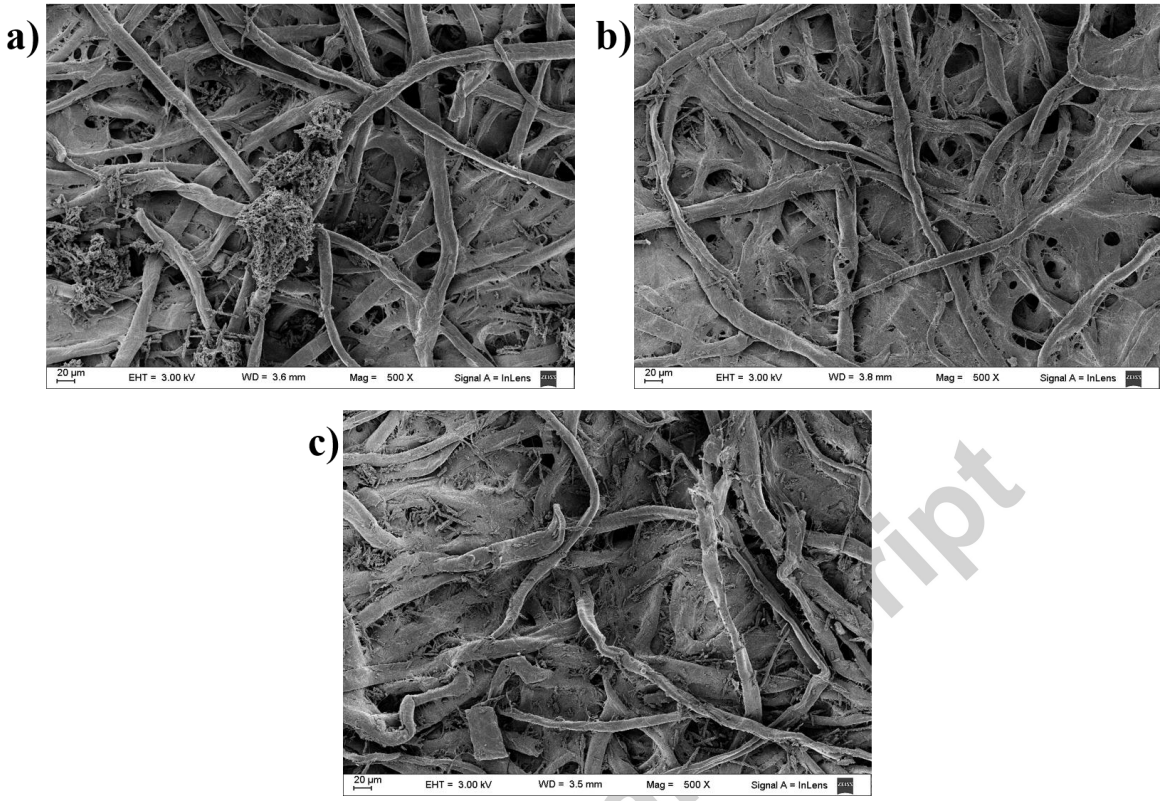
a)
20 µm EHT = 3.00 kV WD = 3.6 mm Mag = 500 X Signal A = InLens
b)
20 µm EHT = 3.00 kV WD = 3.8 mm Mag = 500 X Signal A = InLens
c)
20 µm EHT = 3.00 kV WD = 3.5 mm Mag = 500 X Signal A = InLens

Fig. 2

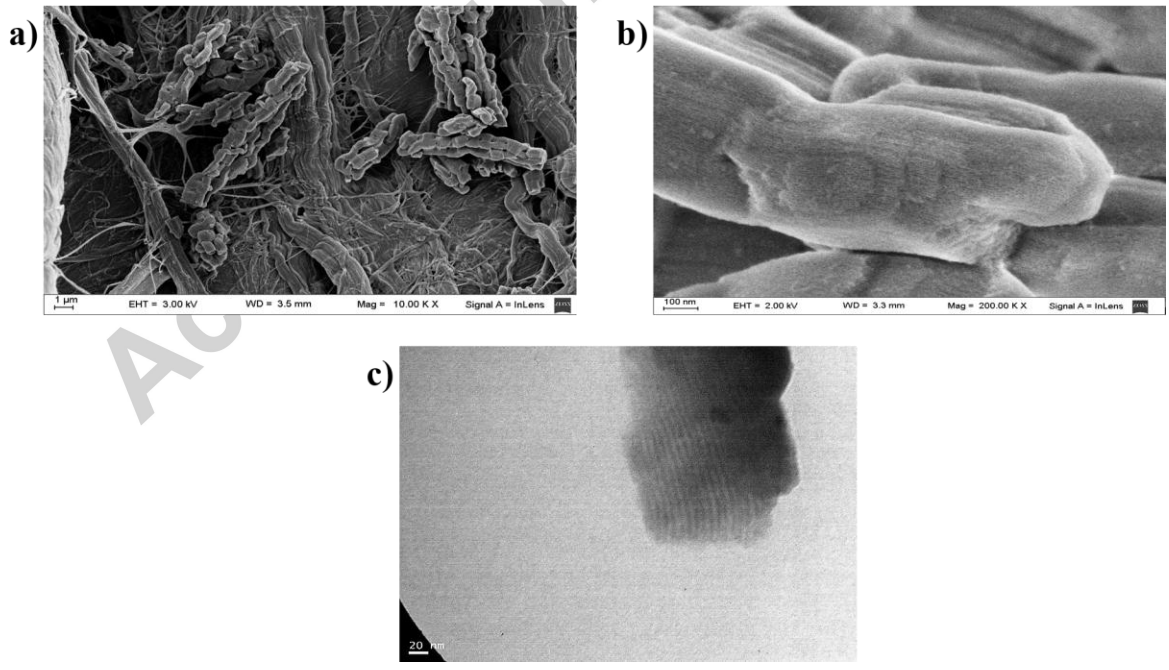
a)
1 µm EHT = 3.00 kV WD = 3.5 mm Mag = 10.00 K X Signal A = InLens
b)
100 nm EHT = 2.00 kV WD = 3.3 mm Mag = 200.00 K X Signal A = InLens
c)
20 nm

Fig. 3

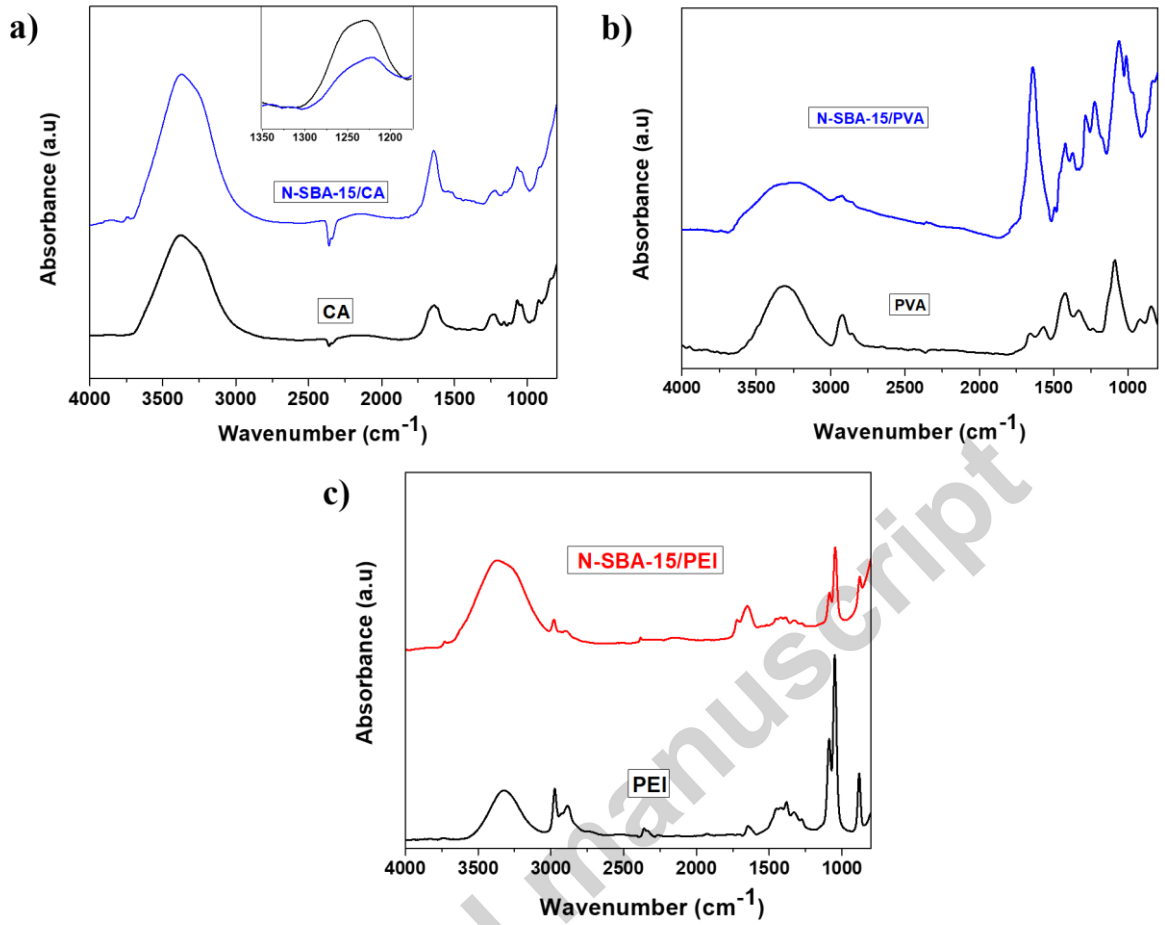
a)
Absorbance (a.u)
N-SBA-15/CA
CA
Wavenumber (cm-1)
b)
N-SBA-15/PVA
PVA
c)
N-SBA-15/PEI
PEI

Fig. 4

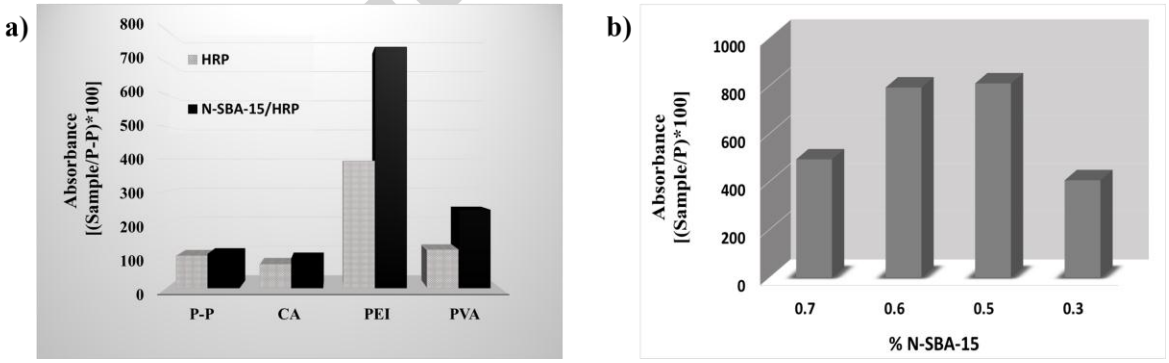
a)
HRP
N-SBA-15/HRP
Absorbance [(Sample/P-P)*100]
P-P
CA
PEI
PVA
b)
Absorbance [(Sample/P)*100]
% N-SBA-15

Fig. 5

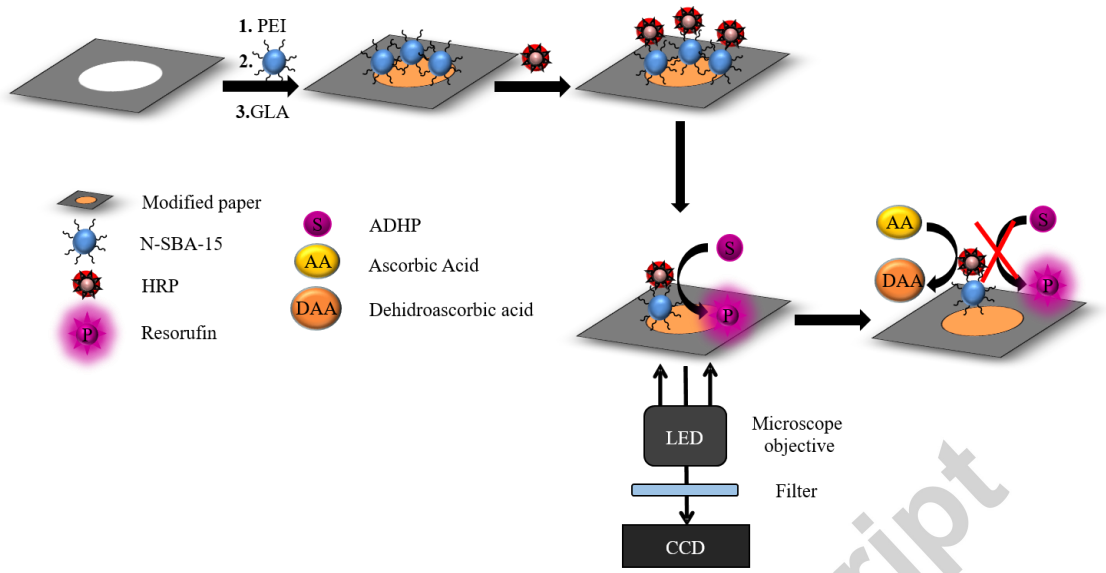

Fig. 6

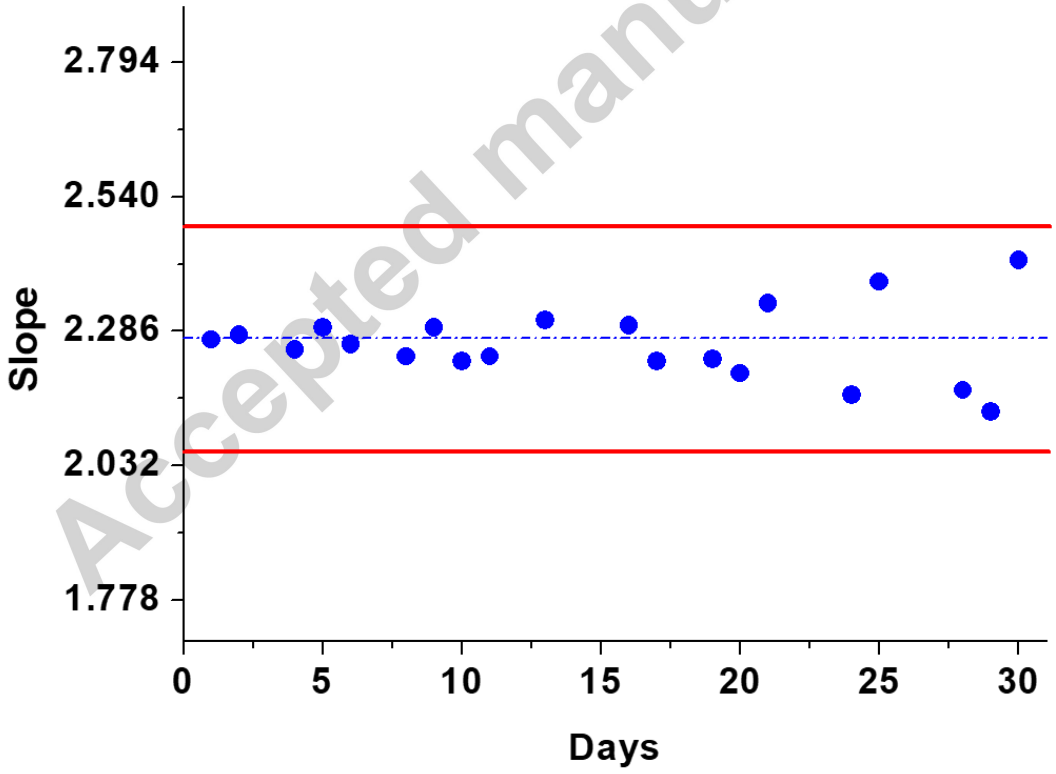

Fig. 7

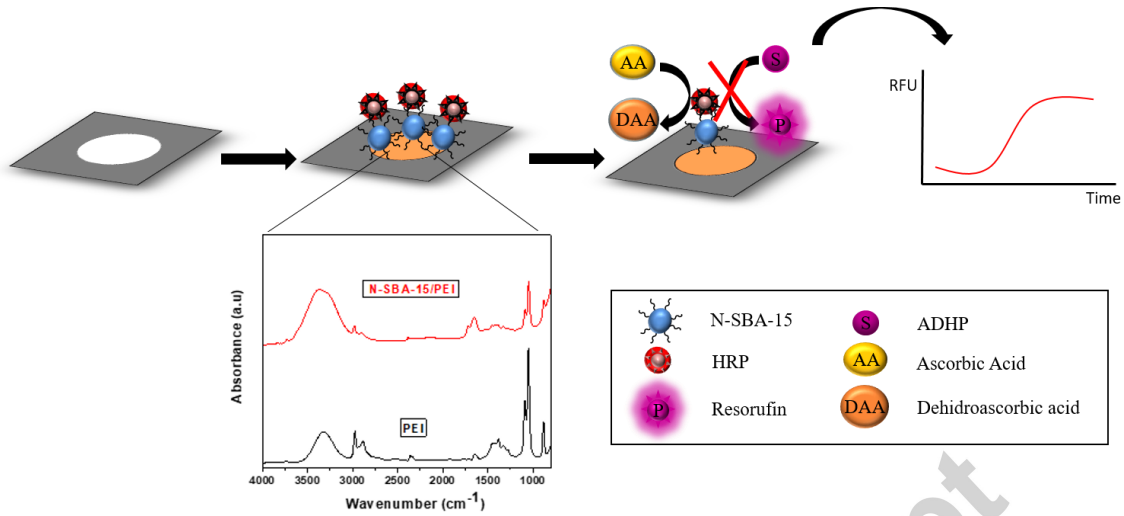

Graphical Abstract

Table 1. AA quantification in pharmaceutical formulations.

Sample	AA[a]	RSD (%)
Redoxon effervescent tablets	1.021 ± 0.035 g	3.43
Redoxon oral drops	0.204 ± 0.009 g mL^{-1}	4.41
Vitamin C injectable	0.202 ± 0.008 g mL^{-1}	3.96
Vitamin C powder	0.987 ± 0.028 g	2.84
Vitamin C tablets	0.509 ± 0.016 g	3.14

[a]Mean of five determinations

Table 2. Comparison of recent methods for the AA determination.

Method	Materials	Linear range (μmol L^{-1})	Detection limit (μmol L^{-1})	Reference
Fluorescence	Graphene quantum dots	1.11-300	0.320	[31]
Fluorescence	Carbon dots-MnO_2	0.5-20	0.068	[32]
Fluorescence	Sulfanilic acid/Glutathione-Graphene quantum dots	0.4-12	0.020	[33]
Fluorescence	Phosphorus/Nitrogen-Carbon quantum dot	5-200	1.35	[34]
Fluorescence	Cu-ZnCdS QDs/MnO_2	5.02-401.77	31.62	[35]
Fluorescence	N-SBA-15/PAD	0.05-1.5	0.015	This method

Highlights

- Different modification strategies are compared to obtain an amine functionalized SBA-15 composite modified paper-based device.
- N-SBA-15/PEI composite shows the highest signal response, providing an excellent platform for the paper biosensors construction.
- This device represents a novel strategy for the paper-based biosensor development.